Manufacturing CD20/CD19-targeted iCasp9 regulatable CAR-T_{SCM} cells using *qCART*, the *Quantum pBac*-based CAR-T system

Running Title: Manufacturing CAR-T_{SCM} cells using *qCART*

Peter S. Chang[1,*], Yi-Chun Chen[1,*], Wei-Kai Hua[1,*] , Jeff C. Hsu[1], Jui-Cheng Tsai[1], Yi-Wun Huang[1], Yi-Hsin Kao[1], Pei-Hua Wu[1], Yi-Fang Chang[2,3,4], Ming-Chih Chang[2], Yu-Cheng Chang[2,3], Shiou-Ling Jian[5], Jiann-Shiun Lai[5], Ming-Tain Lai[5], Wei-Cheng Yang[6], Chia-Ning Shen[6,7], Kuo-Lan Karen Wen[1,†], Sareina Chiung-Yuan Wu[1,†]

[1]GenomeFrontier Therapeutics, Inc. Taipei City, Taiwan (R.O.C.)

[2]Division of Hematology and Oncology, Department of Internal Medicine, Mackay Memorial Hospital, Taipei, Taiwan (R.O.C.)

[3]Department of Medical Research, Laboratory of Good Clinical Research Center, Mackay Memorial Hospital, Tamsui District, New Taipei City, Taiwan (R.O.C.)

[4]Department of Medicine, Mackay Medical College, New Taipei City, Taiwan (R.O.C.)

[5]OBI Pharma, Inc.

[6]Biomedical Translation Research Center, Academia Sinica, Taipei, Taiwan (R.O.C.)

[7]Genomics Research Center, Academia Sinica, Taipei, Taiwan (R.O.C.)

[*]These authors contributed equally to this work and their authorship order is interchangeable

[†]To whom correspondence may be addressed. Sareina Chiung-Yuan Wu, Kuo-Lan Karen Wen; 18F-1, No. 3, Park St., Nangang Dist., Taipei City 11503, Taiwan (R.O.C.); +886-2-26558766;

Email: sareina@genomefrontier.com, klwen@genomefrontier.com

Keywords: multiplex CAR-T | *piggyBac* | T_{SCM} | transposon

List of Abbreviations:

aAPC, artificial antigen presenting cells; CAR, chimeric antigen receptor; CLL, chronic lymphocytic leukemia; CRS, cytokine release syndrome; CT, threshold cycle; DLBCL, diffuse large B-cell lymphoma; EFS, event-free survival; GF-CART01, patient-derived bicistronic CD20/CD19-targeted iCasp9 regulatable CAR-T cells; GMP, good manufacturing practice; GVHD, graft-versus-host disease; HL, Hodgkin lymphoma; ICANS, immune effector cell-associated neurotoxicity syndrome; iCasp9, inducible caspase 9; i.v., intravenously; MM, multiple myeloma; NHL, Non-Hodgkin lymphoma; PBMCs, peripheral blood mononuclear cells; PE, R-phycoerythrin; PFS, progression-free survival; *qCART*, *Quantum CART*; *qPB*, *Quantum pBac*; T_{CM}, central memory T cell; T_{EFF}, effector T cell; T_N, naïve T cell; T_{SCM}, T stem cell memory.

DECLARATIONS:

Ethics approval and consent to participate

Fresh/frozen peripheral blood mononuclear cells (PBMCs) from adult healthy donors and patients were obtained from Chang Gung Memorial Hospital (IRB approval #201900578A3) and MacKay Memorial Hospital (IRB approval #20MMHIS330e), respectively. *In vivo* mouse xenograft model studies were conducted at the Development Center for Biotechnology (Taiwan) using Taiwan Mouse Clinic IACUC (2020-R501-035) approved protocols.

Consent for publication

All authors consent to publication of this manuscript.

Availability of data and material

The authors confirm that the data supporting the findings of this study are available within the article and/or its supplementary materials.

Competing interests

S.C.-Y.W. is the founder of GenomeFrontier Therapeutics, Inc., P.S.C., Y.-C.C. (Chen), W.-K.H., J.C.H., J.-C.T., Y.-W.H., Y.-H.K., P.-H.W., and K.-L.K.W. are affiliated with GenomeFrontier Therapeutics, Inc.

Funding

This study is funded by GenomeFrontier Therapeutics, Inc.

Authors' contributions

S.C.-Y.W. designed research. Y.-C. C. (Chen), J.-C.T., Y.-W.H., Y.-H.K., P.-H.W., Y.-F.C., M.-C.C., and Y.-C. C. (Chang) performed research. P.S.C., W.-K.H., Y.-C. C. (Chen), J.C.H., K.-L.K.W., and S.C.-Y.W. analyzed data. P.S.C., J.C.H., and S.C.-Y.W. wrote the paper.

Acknowledgements

The authors thank Ms. Jin-hwa Yang for her assistance with IRB preparation and approval process. The authors also thank Dr. Pei-Yi Tsai for assistance with the animal experiments.

ABSTRACT

Background: CD19-targeted chimeric antigen receptor therapies (CAR19) have driven a paradigm shift in the treatment of relapsed/refractory B-cell malignancies. However, >50% of CAR19-treated patients experienced progressive disease mainly due to antigen escape and low persistence. Clinical prognosis is heavily influenced by CAR-T cell function and systemic cytokine toxicities. Furthermore, it remains a challenge to efficiently, cost-effectively, and consistently manufacture clinically relevant number of virally engineered CAR-T cells.

Methods: Using a highly efficient *piggyBac* transposon-based vector, *Quantum pBac*, we developed a virus-free cell engineering system, *Quantum CART (qCART™)*, for development and production of multiplex CAR-T therapies.

Results: Here, we demonstrated *in vitro and in vivo* that consistent, robust, and functional CD20/CD19 dual-targeted CAR-T stem cell memory (T_{SCM}) cells can be efficiently manufactured using the *qCART*™ system for clinical application. *qCART*™-manufactured CAR-T cells from cancer patients expanded efficiently, rapidly eradicated tumors, and can be safely controlled via an iCasp9 suicide gene-inducing drug.

Conclusions: The *qCART*™ system is an elegant system for the manufacturing of CAR-T products having all the desired CAR-T therapy attributes. We believe that the simplicity of manufacturing multiplex CAR-T cells using the *qCART*™ system will not only significantly enhance the accessibility of CAR-T therapy but also unlock the full potential of armored CAR-T therapy for the treatment of solid tumors in the future.

What is already known on this topic

Despite the considerable success which has been achieved with CD19-targeted chimeric antigen receptor therapies (CAR19), >50% of CAR19-treated patients still experienced progressive disease. Therefore, there

95 is a need to further improve CAR19 therapies. Current CAR19 therapies commonly utilize virus-based cell
96 engineering methods. CAR-T production using these methods face multiple hurdles, including difficulties
97 to efficiently, cost-effectively, and consistently manufacture clinically relevant number of CAR-T cells. We
98 have previously used a highly efficient *piggyBac* transposon-based vector, *Quantum pBac,* to establish
99 *Quantum CART* (*qCART*™) which is a virus-free cell engineering system for development and production
100 of multiplex CAR-T therapies.

101 **What this study adds**

102 In this report, we further demonstrate *in vitro* and *in vivo* that consistent, robust, and functional iCasp9-
103 regulatable, CD20/CD19 dual-targeted CAR-T stem cell memory (T_{SCM}) cells can be efficiently
104 manufactured using the *qCART*™ system for clinical application. These cells possess all the desired
105 attributes for ensuring therapeutic efficacy in CAR-T therapy, including high CAR-T_{SCM}, balanced CD8/CD4
106 ratio, low exhaustion and senescence marker expressions, and high *ex vivo* and *in vivo* expansion capacity.
107 Importantly, we show that *qCART*™-manufactured CAR-T cells from hematological cancer patients
108 expanded efficiently, effectively eradicated tumors, and can be safely controlled via an iCasp9 suicide
109 gene-inducing drug. We believe that the simplicity of manufacturing multiplex CAR-T cells using the
110 *qCART*™ system will not only significantly enhance the accessibility of CAR-T therapy but also unlock the
111 full potential of armored CAR-T therapy for the treatment of solid tumors in the future.

112 **How this study might affect research, practice or policy**

113 Our findings demonstrate that *qCART*™ is a virus-free CAR-T engineering system for manufacturing CAR-
114 T_{SCM} cells from either healthy donors or hematological cancer patients, that possess all the desired
115 attributes for a successful CAR-T therapy. These cells expanded efficiently, rapidly eradicated tumors, and
116 can be safely controlled via activation of iCasp9. We expect that this simple yet robust system for
117 manufacturing multiplex CAR-T cells will advance the CAR-T field.

118

BACKGROUND

Over the last decade, chimeric antigen receptor (CAR)-T therapy has become one of the most promising cancer treatment, but the heavy reliance on lentiviral and retroviral vectors for CAR-T cell manufacturing makes the therapy expensive and inaccessible to the masses.[1] Frequent cytokine release syndrome (CRS) and immune effector cell-associated neurotoxicity syndrome (ICANS) associated with clinical patients treated with conventional CAR-T therapies have raised safety concerns.[2] Furthermore, virus-based gene therapies have limited gene payload capacity, making them less suitable for engineering multiplex armored CAR-T cells.[3,4]

To date, B-cell malignancies remain the most actively-studied cancers for CAR-T therapy development. Since *Brentjens et al. (2003)* first demonstrated the eradication of B-cell tumors by CD19-targeted second-generation CAR-T cells, several commercial CAR-T products have been approved by FDA.[5,6] However, treatment with CAR19 therapy resulted in only 30-40% long-term progression-free survival (PFS) in aggressive Non-Hodgkin lymphoma (NHL) patients, and the median event-free survival (EFS) of adult B-cell ALL patients was 6.1 months.[7,8] Evidence suggest that downregulation of CD19 may in part be responsible for patient relapse.[9,10] As demonstrated by recent clinical studies, bispecific CD19/CD20-targeted CAR-T therapy improved patient survival compared to CAR19 therapy.[11,12]

Transposon system, such as *Sleeping Beauty* and *piggyBac*, is a virus-free alternative for generating CAR-T cells but suffers from low gene transfer efficiency and limited expansion of engineered cells.[3,13,14] We recently developed the most advanced version of *piggyBac* known as *Quantum pBac (qPB)* that is 15 times more active than *hyperactive piggyBac* in human T cells.[15,16] We previously developed a novel genetic engineering system known as *Quantum CART (qCART™)* that combines efficient transgene design, evaluation, and identification of lead construct (*GTailor*); virus-free vector (*Quantum pBac*); effective gene delivery (*Quantum Nufect*); and optimized cell expansion (*iCellar*).[15,16] We reported that *qCART™* could be used to engineer highly potent T stem cell memory (T_{SCM}) CAR-Tcells. Here,

143 we further validate that the *qCART*™ system can be used to rapidly manufacture highly potent patient-
144 derived bicistronic CD20/CD19-targeted iCasp9 regulatable CAR-T cells (GF-CART01) for treating B-cell
145 malignancies. We demonstrate enhanced anti-tumor efficacy of GF-CART01 cells both *in vitro* and in a
146 xenotransplant immunodeficient mouse model.
147

148 **METHODS**

149 **Cell engineering**

150 CD19-expressing K562 cells were generated by using a *piggyBac*-based cell engineering
151 system. K562 cells were nucleofected using *Quantum Nufect*™ (GenomeFrontier Therapeutics)
152 with a plasmid carrying CD19 and hygromycin genes followed by hygromycin selection for 14
153 days. To select for clones that homogeneously express CD19, limiting-dilution was carried out to
154 reach a concentration of one cell/well. Following clonal expansion, the clone containing the
155 highest % of $CD19^+$ cells was identified and expanded for storage.

156 **Generation/expansion of CAR-T cells**

157 Frozen peripheral blood mononuclear cells (PBMCs) from adult healthy donors and
158 patients were obtained from Chang Gung Memorial Hospital (IRB approval #201900578A3) and
159 MacKay Memorial Hospital (IRB approval #20MMHIS330e), respectively. PBMCs were extracted
160 using Ficoll-Hypaque gradient separation (Cytiva). Primary human $CD3^+$ T cells were isolated from
161 PBMCs by negative selection using EasySep Human T Cell Isolation Kit (StemCell Technologies) or
162 by positive selection using Dynabeads Human T-Expander CD3/CD28 (Thermo Fisher), followed
163 by activation of isolated T cells with Dynabeads (3:1 bead-to-cell ratio) for two days. An iCasp9-
164 CD20/CD19-CAR transposon minicircle carrying CD20 scFv[17] and CD19 scFv[18] and a *qPBase*
165 plasmid were delivered into activated T cells using 4D-Nucleofector device (Lonza) and *Quantum*

166 *Nufect* Kit (GenomeFrontier Therapeutics) according to the manufacturer's instructions.
167 Irradiated artificial antigen presenting cells (aAPC), CD19-expressing K562 cells, were added to
168 electroporated T cells at 1:1 ratio on day 3. Cells were cultured in OpTmizer medium (Thermo
169 Fisher) supplemented with *Quantum Booster* (GenomeFrontier Therapeutics) in G-Rex 24- or 6M-
170 well plates (Wilson Wolf) or conventional plates for 10 days. For lentiviral CAR-T production,
171 cryopreserved human PBMCs were thawed and primary human $CD3^+$ T cells were isolated from
172 PBMCs by using human Pan T Cell Isolation Kit (Miltenyi Biotec, 130-096-535). Cells were
173 activated and expanded with Dynabeads at 1:1 ratio. After 2 days, cells were transduced with 1
174 MOI of concentrated virus containing 8 ug/mL Polybrene (Merck, TR-1003-G). Two days later,
175 Dynabeads were removed and the medium (supplemented with IL-7 and IL-15) was changed
176 every 2-3 days until day 10 when CAR-T cells were cryopreserved.

177 **Cell culture conditions**

178 **Fed-batch**: On day 1, approximately $1x10^5$ nucleofected cells were seeded into a well of 24-well
179 G-Rex containing 3 ml of medium. Fresh medium (2ml) was added on days 3 and 5. On day 7,
180 culture was replaced with fresh medium (2ml).

181 **Perfusion**: On day 1, nucleofected cells were seeded into conventional 24-well plates at a
182 concentration of $2.5x10^5$ cells/ml. Every 2 to 3 days, the cell numbers were counted, medium was
183 added to adjust the concentration to $2.5x10^5$ cells/ml, and cells were placed back into culture
184 (depending on the volume, up to a 10 ml flask was used to culture these cells).

185 For both of these culture approaches, cells were harvested on day 10 to be used for subsequent
186 experiments.

187

188 **Flow cytometry**

189 CAR expression on T cells was analyzed by co-incubating cells with a Biotin-SP (long
190 spacer) AffiniPure F(ab')$_2$ Fragment Goat Anti-Mouse IgG antibody (Jackson ImmunoResearch)
191 for 30 min at 4°C and R-phycoerythrin (PE)-conjugated streptavidin (Jackson ImmunoResearch)
192 for 30 min at 4°C. Expression of surface molecules of T cells were determined by labeling T cells
193 with fluorochrome conjugated monoclonal antibodies: CD4-AlexaFlour532 (Thermo Fisher), CD3-
194 Pacific Blue, CD3-PE-Cy5, CD4-AlexaFluor532, CD4-AlexaFlour700, CD8-BV605, CD8-PE-Cy7, CD8-
195 Pacific Blue, CD27-PE-Cy7, CD28-APC, CD45RA-BV421, CD45RO-PE, CD62L-PE-Cy5, CD62L-PE-
196 Dazzle 594, CD95-BV711, CD197-BV510, CD279/PD-1-PE/Cy7, CD366/Tim-3-BV650, CD223/LAG-
197 3-BV711, KLRG-1-BV-421, CD57-PerCP-Cy5.5, CD19-PE, CD56-BV711 (BioLegend), CD45RA-
198 BUV737, and CD95-BUV395 (BD Biosciences). Ghost dye Red 780 fixable viability dye (Cytek),
199 7AAD or propidium iodide (PI) was used to distinguish live cells from dead cells for data analysis.
200 Mouse blood cell samples were stained with anti-hCD45-APC antibody (BioLegend). For counting
201 the absolute cell number, CountBright™ Absolute Counting Beads (Invitrogen, C36950) were
202 added into FACS samples before acquisition by flow cytometry. Flow cytometric data were
203 acquired on an SA3800 Spectral Analyzer (Sony), a BD FACSCantoTM II (BD Bioscience), or a BD
204 LSRFortessa analyzer (Sony). The graphs were generated using GraphPad Prism or FlowJo
205 software (BD Biosciences or Tree Star).

206 **Processing mouse blood samples**

207 100μl of blood/mouse was collected in EDTA-containing tubes by submandibular blood
208 collection. After centrifugation at 3000 x g for 15 minutes, plasma (upper layer) was collected for
209 ELISA. The cell pellets/red blood cells (lower layer) were then resuspended with the RBC Lysis

210 Buffer (Biolegend, cat.420301) for 15 minutes at room temperature. Cell pellets were then
211 centrifuged (350 x g for 5 minutes) and washed once with PBS. These cells were used for DNA
212 extraction. For NCI-N87 tumor model experiments, submandibular blood was collected from
213 mice in MiniCollect® tube (K3EDTA, Greiner) and RBC lysed by ACK buffer (Gibco). These cells
214 were used for FACS analysis.

215 **Enzyme-linked immunosorbent assay (ELISA)**

216 For *in vitro* assay, supernatant was collected 24 hours after CAR-T and Raji-GFP/Luc cell
217 (Creative Biogene, Cat. No: CSC-RR0320) co-culture (E:T=1:1). For *in vivo* assay, mouse plasma
218 samples were collected on days 2, 5, 8, and 14 after T cell injection. IFN-γ (Thermo Fisher), TNF-
219 α (Thermo Fisher), IL-6 (Thermo Fisher), and IL-2 (BioLegend) were quantified by ELISA according
220 to manufacturer's instructions.

221 **Genomic DNA extraction and quantitative PCR (qPCR)**

222 Genomic DNA from mouse blood was extracted using a DNeasy Blood & Tissue Kit
223 (Qiagen) following the manufacturer's instructions. For qPCR analysis, CAR-T cells and Raji-
224 GFP/Luc cells were assessed using the following primer sequences: CAR: fwd-5'-
225 ACGTCGTACTCTTCCCGTCT-3', rev-5'-GATCACCCTGTACTGCAACCA-3'; Luciferase: fwd-5'-
226 GGACTTGGACACCGGTAAGA-3', rev-5'-GGTCCACGATGAAGAAGTGC-3'. All qPCR assays were
227 performed using a 7500 fast real-time PCR system (Applied Biosystems). Absolute transgene
228 levels were calculated using the standard curve method. The threshold cycle (CT) value of each
229 target was converted to a concentration using the appropriate standard curve and calculating
230 the % of cells in mouse blood based on the cell copy number.

231

232 ***In vitro* cytotoxicity assay**

233 Cytotoxicity was assessed using Celigo image cytometry (Nexcelom). Raji-GFP/Luc target
234 cells were seeded in 96-well culture plates. CAR-T cells were then added at E:T ratios of 5:1, 1:1,
235 and 1:5. At 0, 24, 48, 72, and 96 hours after cell co-culture, Raji-GFP/Luc cells were quantified.
236 The % specific lysis was calculated from each sample using the formula [1-(live fluorescent cell
237 count in target-effector cell co-culture/ live fluorescent cell count in target cell only culture)] x
238 100.

239 **Anti-tumor efficacy in mouse tumor models**

240 *In vivo* mouse xenograft model studies were conducted at the Development Center for
241 Biotechnology (Taiwan) using Taiwan Mouse Clinic IACUC (2020-R501-035) approved protocols.
242 Six to eight-week-old male immunodeficient (NOD.Cg-Prkdc^{scid}Il2rg^{tm1Wjl}/YckNarl) mice (National
243 Laboratory Animal Center, Taiwan) were engrafted with 1.5x10^5 Raji-GFP/Luc tumor cells
244 intravenously (*i.v.*) or with Matrigel (1:1, BD Bioscience) containing 2x10^6 NCI-N87-Luc cells
245 subcutaneously (*s.c.*) on the right flank. For Raji tumor model experiments, mice were infused
246 one week later with 7.5x10^5 (low), 3x10^6 (medium), or 1x10^7 (high) CAR-T cells from donor PBMC-
247 41. After 35 days, 1.5x10^5 Raji-GFP/Luc tumor cells were injected (*i.v.*) to half of the mice in each
248 group. Raji-GFP/Luc tumor cells were quantified using the Xenogen-IVIS Imaging System (Caliper
249 Life Sciences). For NCI-N87 tumor model experiments, mice were injected *i.v.* 11 days later with
250 4x10^6 control or CAR-T cells. Mice were imaged on an Ami-HT optical imaging system (Spectral
251 Instruments Imaging), following an intraperitoneal (*i.p.*) injection of D-Luciferin (BIOSYNTH, L-
252 8220)

253

254 ***In vitro* iCasp9 safety assay**

255 Activation of inducible caspase 9 (iCasp9) was performed *in vitro* with 2.5, 5, or 10 nM of
256 dimerizer (AP1903), and CAR-T cell elimination was assessed by flow cytometry 24 hours later.

257 **ddPCR copy number assays**

258 Genomic DNA (gDNA) was extracted from GF-CART01 cells using a Qiagen DNeasy Blood
259 and Tissue Kit (Qiagen). Minicircle DNA (positive control) was produced by Aldevron. Before
260 ddPCR, the minicircle DNA was digested for 1 min at 37°C with BsrGI. The reaction for ddPCR
261 Copy Number Variation Assay was set up in 20 µl sample volume containing 10 µl of 2X ddPCR
262 Supermix (no dUTP, BioRad), 1 µl of FAM-labeled target primers/probe (BioRad), 1 µl of HEX-
263 labeled reference primers/probe (BioRad), 0.1 µl of BsrGI (Thermo Fisher), and 50 ng of gDNA or
264 minicircle DNA (volume 2 µl). Nuclease-free water was used to adjust the sample to final volume.
265 *RPP30* was used as housekeeping gene. BsrGI directly digests in the ddPCR reaction during setup.
266 Droplets were then generated in a QX200 droplet generator (BioRad) according to
267 manufacturers' instructions with a final volume of 40 µl. DNA amplification was carried out and
268 droplets were analyzed in a QX200 droplet reader (BioRad). Data was analyzed with QuantaSoft
269 software (BioRad).

270 **Statistical analysis**

271 Statistical analysis was performed using GraphPad Prism 7 software. Two-tailed unpaired
272 t-tests were used for comparison of two groups. One-way ANOVA was used for comparison of
273 three or more groups in a single condition. P values of less than 0.05 were considered statistically
274 significant, $*p < 0.05$, $**p < 0.01$, and $***p < 0.001$.

275

276 **RESULTS**

277 **Comparison of fed-batch (G-Rex) and perfusion (conventional)-cultured CAR-T cells**

278 To assess the potential of *qCART*™ system for CAR-T therapy development, we constructed a
279 second-generation bicistronic CAR (GF-CART01) containing binding domains that recognize CD20 and
280 CD19, human 4-1BB and CD3ζ signaling domains, and iCasp9 suicide gene driven by the EF1α promoter
281 **(Figure 1A)**. Following nucleofection of GF-CART01 DNA, we expanded CAR-T cells in G-Rex (fed-batch)
282 and conventional (perfusion) plates. The percentage of CAR^+ T cells in the fed-batch-cultured (46%) and
283 perfusion-cultured (51%) CAR-T cells were comparable **(Figure 1B)**. However, we observed significantly
284 higher expansion of perfusion-cultured CAR-T cells (836-fold) compared to fed-batch-cultured CAR-T cells
285 (189-fold). Notably, both the perfusion- and fed-batch-cultured CAR-T cells had a high percentage of
286 $CD45RA^+CD62L^+CD95^+$ T_{SCM} among the CAR^+ CD4 and CD8 populations. Despite noticeable lower
287 proliferation of fed-batch compared to perfusion-cultured CAR-T cells, we observed enhanced anti-tumor
288 cytotoxicity in fed-batch-cultured CAR-T cells **(Figure 1C)**. As G-Rex will be adopted for good
289 manufacturing practice (GMP) CAR-T manufacturing, all subsequent experiments were conducted in G-
290 Rex.

291 **Safety assessment of GF-CART01 cells**

292 To better manage CAR-T therapy-associated adversities, we included an iCasp9 suicide gene in
293 the GF-CART01 construct. We demonstrated that AP1903 treatment, which activates iCasp9, resulted in
294 a significant reduction in GF-CART01 cell survival **(Supplementary Figure S1A)**. To comply with GMP safety
295 standards for CAR-T manufacturing, we need to ensure that GF-CART01 cells have low integrant (CAR)
296 copy number per cell (<5). We have previously demonstrated that increasing the concentration of DNA
297 for electroporation increased CAR^+ T cells in a dose-dependent manner (data not shown). Here, we
298 modified CAR-T cells using different amounts of GF-CART01 DNA and determined that the CAR copy
299 number remained low (<5) when 15 μg of total DNA was used for nucleofection **(Supplementary Figure**

300 **S1B)**. All subsequent experiments were conducted using 15 µg of DNA per $5x10^6$ cells to maximize
301 generation of CAR^+ T cells while maintaining safety levels of CAR DNA copy numbers.

302 **GF-CART01 cells are dominated by T_{SCM} cells with high proliferative capacity and low expression of**
303 **exhaustion and senescence markers**

304 We next examined the proliferative capacity of GF-CART01 cells generated from 9 independent
305 healthy donors and monitored CAR expression on days 1, 8, and 10 following nucleofection. We observed
306 a mean basal level of 21.49% CAR^+ T cell population on day 1, which subsequently increased and stabilized
307 at 55.7% and 56.75% on days 8 and 10, respectively **(Figure 2A)**. As the presence of transposase (*Quantum*
308 *PBase*, or *qPBase*) in modified T cells may lead to genotoxicity long-term, we also monitored the *qPBase*
309 levels following nucleofection. While the *qPBase* levels were high on day 1 (47.31%), only a minimal (<0.2%)
310 fraction of *qPBase*$^+$ cells was observed on days 8 and 10, suggesting that concerns regarding *qPBase*-
311 induced integrant remobilization should be minimal **(Figure 2B).** We also observed an average of 178.86-
312 fold GF-CART01 cell expansion **(Figure 2C)**.

313 Among the donors, we consistently observed a higher CD8 (73.58%) compared to CD4 (21.98%)
314 CAR^+ population **(Figure 2D)**. To assess the composition of GF-CART01 cells, we determined the
315 percentage of $CD45RA^+CD62L^+CD95^-$ naïve T cell (T_N), $CD45RA^+CD62L^+CD95^+$ stem cell memory T cell (T_{SCM}),
316 $CD45RA^-CD62L^+CD95^+$ central memory T cell (T_{CM}), $CD45RA^-CD62L^-CD95^+$ effector memory T cell (T_{EM}), and
317 $CD45RA^-CD62L^-CD95^-$ effector T cell (T_{EFF}) subsets in the CD4 and CD8 CAR^+ populations. We observed high
318 percentage of CAR-T_{SCM} cells in both the CD4 (68.94%) and CD8 (79.84%) populations compared to the
319 other T cell subsets **(Figure 2E)**. Furthermore, these CAR-T cells displayed low exhaustion (PD-1, TIM-3,
320 and LAG-3) markers and the senescence marker CD57 expression **(Figure 2F and G)**. Interestingly, a small
321 but significant population (~9.92%) expressed the senescence marker KLRG-1.

322 **GF-CART01 cells display robust cytotoxic function and distinct proliferative responses to CD19- and**
323 **CD20-expressing target cells**

We next tested the anti-tumor function of GF-CART01 cells in two independent donors, PBMC-41 and PBMC-40. Raji-GFP/Luc tumor cells were co-cultured with GF-CART01 cells at effector to target (E:T) ratios of 5:1, 1:1, and 1:5, and cytotoxicity was assessed at 24, 48, 72, and 96 hours after co-culture **(Figure 3A and B)**. While GF-CART01 cells lysed Raji-GFP/Luc tumors in a dose-dependent manner at early time points (24 to 48 h), complete tumor lysis was seen in all E:T ratios at 96 hours. Furthermore, GF-CART01 cells secreted significant levels of pro-inflammatory cytokines IFN-γ, TNF-α, and IL-2 compared to pan-T cells **(Figure 3C-E)**. Collectively, these data suggest that functional GF-CART01 cells can be generated using the *qCART*™ system. Next, we determined how encountering different antigen levels may affect the proliferation capacity of GF-CART01 cells. To address this question, eF450 dye-labeled GF-CART01 cells were co-cultured with K562 cells overexpressing different levels of CD19 or CD20 and proliferation capacity assessed at 48 and 72 hours (see **Supplementary Figure S2** for gating strategy). As shown in **Table 1**, the percentage of proliferated GF-CART01 cells was inversely associated with CD19 expression, but positively associated with CD20 expression, on K562 cells. No such association was observed with CAR$^-$ T cells in the corresponding groups and CAR-T cell viability did not appear to be negatively affected by CD19 or CD20 expression (data not shown).

Table 1. Proliferation capacity of GF-CART01 cells in response to K562 expressing different levels of CD19 or CD20 antigens. Percentages of proliferated live CAR+ and CAR- GF-CART01 cells following 48 h and 72 h co-culture with different levels of CD19- or CD20-overexpressing K562 clones are shown.

		CAR$^+$				CAR$^+$			
		% Proliferated				% Proliferated			
	Target cell	K562	K562-CD19 #4-B10 (low)	K562-CD19 #7-B8 (medium)	K562-CD19 #2D-4 (high)	K562	K562-CD20 #4-2 (low)	K562-CD20 #5-2 (medium)	K562-CD20 #3-2 (high)
Time of co-culture	48 hours	4.8 ± 1.7	28.7 ± 2.4	24.9 ± 0.6	19.5 ± 1.5	7.6 ± 0.8	12.5 ± 1.2	13.5 ± 0.7	11.9 ± 1.3
	72 hours	27.6 ± 1.0	77.5 ± 1.3	69.3 ± 1.9	63.9 ± 0.1	10.4 ± 0.2	60.4 ± 3.0	74.7 ± 2.3	72.7 ± 2.0
		CAR$^-$				CAR$^-$			
		% Proliferated				% Proliferated			
	Target cell	K562	K562-CD19 #4-B10 (low)	K562-CD19 #7-B8 (medium)	K562-CD19 #2D-4 (high)	K562	K562-CD20 #4-2 (low)	K562-CD20 #5-2 (medium)	K562-CD20 #3-2 (high)
Time of co-culture	48 hours	2.2 ± 2.0	12.6 ± 1.6	13.9 ± 0.9	11.3 ± 0.3	4.7 ± 0.9	5.5 ± 2.2	5.6 ± 0.7	7.2 ± 3.2
	72 hours	19.0 ± 1.4	44.9 ± 2.6	50.3 ± 1.3	46.3 ± 0.3	6.9 ± 0.8	28.1 ± 2.1	31.9 ± 0.7	25.6 ± 0.5

343 % of CAR+ cells (stained by anti-mouse IgG Fab') were detected by flow cytometry (SonySA3800) All results were
344 obtained in triplicates

345 **GF-CART01 cells display enhanced and persistent anti-tumor function *in vivo***

346 We next evaluated the anti-tumor efficacy of GF-CART01 cells in an *in vivo* xenotransplant
347 immunodeficient mouse model using donor PBMC-41. We injected $1.5x10^5$ Raji-GFP/Luc tumor cells
348 intravenously (*i.v.*) followed by $7.5x10^5$ (low), $3.0x10^6$ (medium), or $1x10^7$ (high) GF-CART01 cells (*i.v.*) 7
349 days later as depicted in **Figure 4A**. As assessed by bioluminescence, all mice in the vehicle group
350 succumbed to tumor by day 21 **(Figure 4B-C)**. In contrast, Raji-GFP/Luc tumors were dose-response
351 dependently cleared and all tumors were completely eradicated by day 13 in all three treatment groups
352 and remained tumor-free **(Figure 4B)**. Minimal cytokine production was detected in all three treatment
353 groups on days 2, 8, and 14 **(Supplementary Figure S3A)**. On day 26, no detectable levels of Raji-GFP/Luc
354 tumors were observed in all three treatment groups **(Supplementary Figure S3B)**. Moreover, residual CAR
355 gene was observed in the blood of the medium and high groups, suggesting that many GF-CART01 cells
356 persisted to form memory T cells **(Supplementary Figure S3C)**. We also obtained data from mice injected
357 with non-transfected control Pan-T cells that were cultured under the same conditions as the GF-CART01
358 cells (**Supplementary Figure S4**). These cells exhibited anti-Raji activity approximately two weeks
359 following injection, which likely resulted from *in vivo* expansion of cells that recognized (and killed) Raji
360 tumor cells via a CAR-independent, TCR-mediated mechanism. However, such a killing effect would not
361 be expected with autologous T cell therapy in patients.

362 While residual GF-CART01 cells (as determined by qPCR for presence of CAR gene in genomic DNA
363 of mouse blood samples) can be detected up to day 26, it remained unclear whether these residual cells
364 were memory T cells and retained their anti-tumor function. To address this, we rechallenged half of the
365 mice in each treatment group with $1.5x10^5$ Raji-GFP/Luc tumor cells on day 35. Due to the lack of CAR-T
366 cell persistence, most of the rechallenged mice in the low group eventually succumbed to tumor **(Figure**

367 **4B-C)**. In contrast, the rechallenged mice in the medium and high groups remained tumor-free throughout
368 the experiment. Some mice in the medium and high groups did not survive, but this was likely due to graft-
369 versus-host disease (GVHD) as severe ruffling were observed in these mice. More importantly, GF-CART01
370 cell treatment significantly improved the overall survival of tumor-bearing mice compared to vehicle
371 control **(Figure 4D)**.

372 To confirm that our non-viral gene engineering approach produces CAR-T cells of high quality and
373 quantity, we next directly compared our non-viral *qCART*™ system with a conventional lentiviral
374 engineering approach. CAR-T cells derived from the same healthy donor PBMC source carrying a CAR
375 gene targeting to a pan-cancer antigen was produced utilizing both approaches. The anti-tumor effects of
376 these CAR-T cells were determined in mice harboring NCI-N87 gastric carcinoma xenografts. The rationale
377 for choosing a single CAR gene targeting to a solid tumor model system was two-fold: First, since the
378 transgene size of GF-CART01used in the Raji tumor model animal experiments was 5.2 Kb (**Figure 4**), CAR-
379 T production using a viral vector system expressing such a sizable transgene would be difficult and may
380 introduce additional variables influencing the results. Second, comparisons carried out in a solid tumor
381 model would be expected to better differentiate between the differences in quality of the CAR-T cells
382 produced using *qCART*™ and the lentivirus systems, since solid tumors are more challenging to be
383 eliminated. We demonstrated that *qCART*™ produced CAR-T cells were superior in performance
384 compared to lentivirally-engineered CAR-T cells, characterized by greater *in vitro* expansion capacity,
385 higher CD8/CD4 ratio, and enrichment of CAR-T_{SCM} cells **(Supplementary Table S1)**. More importantly, in
386 the solid tumor NCI-N87 xenotransplant model **(Figure 4E)**, we observed enhanced antitumor efficacy as
387 well as *in vivo* expansion of *qCART*™-produced CAR-T cells. This was characterized by complete clearance
388 of tumors at Day 28 **(Figure 4F)** in mice treated with *qCART*™-produced CAR-T cells but not those treated
389 with lentivirus-engineered counterparts. Furthermore, between 10 and 37 days following CAR-T injection
390 (CAR-T cells injected at 11 days following tumor inoculation), circulating CAR-T cells robustly proliferated

391 in mice (10 to 100 fold increase in circulating CAR-T cells), while lentivirus-produced CAR-T cells either
392 minimally proliferated or did not proliferate at all **(Figure 4G)**. This difference may reflect the above-
393 mentioned higher CD8/CD4 ratio and percentage of T_N/T_{SCM} population present in both the $CD4^+$ and $CD8^+$
394 CAR-T populations of *qCART*™-produced CAR-T cells **(Supplementary Table S1)**.

395 **Functional GF-CART01 T_{SCM} cells can be generated in sufficient numbers from cancer patients**

396 We next assessed whether sufficient high-quality GF-CART01 cells can be generated for clinical
397 applications. In our previous experiments thus far, we expanded all GF-CART01 cells with CD19-expressing
398 aAPC. To streamline the manufacturing process, we tested whether we can still generate highly potent
399 patient-derived GF-CART01 T_{SCM} cells in the absence of aAPC selective expansion. We isolated PBMCs from
400 6 healthy donors, 3 diffuse large B-cell lymphoma (DLBCL) patients, 3 chronic lymphocytic leukemia (CLL)
401 patients, one Hodgkin lymphoma (HL) patient, and one multiple myeloma (MM) patient to generate GF-
402 CART01 cells. **Figure 5** and **Table 2** summarize the characteristics of the healthy donor- and patient-
403 derived CAR-T cells.

404

405

406

407

408

409

410

411

412

413

414

415 **Table 2. Comparison of GF-CART01 cells generated from healthy donors and cancer patients**

Disease		Healthy Donor	DLBCL1	DLBCL2	DLBCL3	CLL1	CLL2	CLL3	HL	MM
Copy Number		1.85-3.47	2.51	5.46	2.21	3.36	2.81	3.76	2.04	1.82
% of CAR$^+$		32.5–49.6	26.3	50.1	34.23	40.6	33.4	53.22	26.2	19.9
Fold Expansion		43.54–157.55	67.22	67.3	60.38	104.6	58.0	198.96	149.75	139.35
Cell Number (x10^6)		17.34–50.60	7.29	4.95	5.8	15.8	7.71	4.58	24.08	27.54
% of B Cells (CD19$^+$)		0.01-0.36	0.77	1.18	0.35	0	0	0.61	0	0
% of NK Cells (CD3$^-$, CD56$^+$)		0.04-0.27	0.06	2.69	0.63	0.03	0.02	0.02	0.08	0.05
% of Exhaustion Marker$^+$ Cells	PD-1	0.40–1.96	5.4	4.2	4.2	1.0	2.4	6.0	1.7	7.8
	TIM-3	0.10–5.34	1.8	3.0	2.0	1.4	2.3	2.4	1.4	1.1
	LAG-3	0.90–7.00	9.9	12.4	22.8	3.2	4.0	2.6	2.4	2.6
% of Senescence Marker$^+$ Cells	KLRG-1	2.24–14.61	11.8	14.7	8.2	2.8	4.2	6.1	4.1	5.3
	CD57	0.03–0.68	5.8	1.5	2.5	1.1	1.8	0.6	1.1	1.3
Potency (% of lysis) (fresh cells, E/T=5, 48 h)		89.74–95.38	99.66	99.7	99.7	99.88	99.45	99.07	98.96	99.42
Potency (% of lysis) (frozen cells, E/T=5, 48 h)		44.99–61.96	73.35	74.21	75.21	84.30	75.70	45.46	77.49	70.31

416

417 CAR-T cells generated from PBMCs of 6 healthy donors and 8 cancer patients were cultured in 24-well G-Rex for 10
418 days. The cell number of 24-well G-Rex culturing times 50 is equal to cell number of 1 L G-Rex culturing (2.29x10^8-
419 1.38x10^9 cells in 1 L G-Rex). DLBCL: diffuse large B-cell lymphoma; CLL: chronic lymphocytic leukemia; HL:
420 Hodgkin lymphoma; MM: multiple myeloma.

421

422 Over the course of 10 days, we expanded the CAR-T cells to 4.58x10^6–2.76x10^7 cells in a 24-well
423 G-Rex culture, which would be equivalent to clinically relevant number of 2.29x10^8–1.38x10^9 cells in a 1 L
424 G-Rex culture vessel. The CAR expression (19.9–53.22%) and the fold expansion (58.0–198.96 folds) of the
425 patient cells were comparable to those from healthy donors (32.5–49.6% and 43.54–157.55 folds) **(Table**
426 **2)**. The CAR-T cell purity was confirmed by the low percentage of CD19$^+$ B cells and CD3$^-$CD56$^+$ NK cells in
427 both the healthy donors (0.01-0.36% B; 0.04-0.27% NK) and patient cells (0-1.18% B; 0.02-2.69% NK)

428 **(Table 2)**. The proportion of CD8 and CD4 were balanced in both the healthy donors (CD8/CD4=0.85) and
429 the patients (CD8/CD4=1.17) prior to nucleofection **(Figure 5A)**. After nucleofection, the CAR-T cells from
430 healthy donors had higher CD8/CD4 ratio (5.64). However, the increase in the proportion of CAR^+ CD8 T
431 cells was only observed in some patients **(Figure 5A)**. Notably, compared to pre-nucleofection (PBMC)
432 levels, the percentages of T_{SCM} subset at 10 days post-nucleofection increased in all patients among the
433 CD4 (from 13.75% to 76.25%) and CD8 (from 7.17% to 81.90%) populations, confirming the unique quality
434 of *qCART*™ system in supporting T_{SCM} differentiation **(Figure 5B,** see **Supplementary Figure S5** for gating
435 strategy**)**. To further confirm T_{SCM} status, we determined the expression of additional surface antigen
436 biomarkers whose expression have previously been reported to be associated with T_{SCM} and compared
437 their expression among the T_{SCM} ($CD45RA^+CD62L^+CD95^+$) population of PBMC T cells and CAR-T cells
438 derived from three patients and healthy volunteers (**Supplementary Figure S6**). Consistent with data
439 presented in **Figure 2E** and **Figure 5B**, after engineering and expansion, both the patients' and healthy
440 volunteers' (CD4 and CD8) CAR-T cells were highly enriched for T_{SCM} (**Supplementary Figure S6A**). High
441 percentage of these T_{SCM} cells also co-expressed CD45RO, CCR7, CD27 and CD28, confirming these cells'
442 T_{SCM} status (**Supplementary Figure S6C-S6D**). Notably, the $CD45RO^{dim}$ population in these T_{SCM} cells may
443 represent cells that were in transition into a more differentiated state. Furthermore, we also found that
444 the T_N/T_{SCM} population of (particularly healthy donor) PBMCs contained only low percentage of $CD95^+$ cells
445 (**Supplementary Figure S6B**), suggesting that the T_N/T_{SCM} population of PBMCs were dominated by naïve
446 T cells. The GF-CART01 cells were also assessed for expression of exhaustion markers PD-1 and TIM-3 and
447 senescence marker CD57, and only a low percentage of cells were found to express these markers **(Table**
448 **2)**. In addition, the percentage of cells expressing the exhaustion marker LAG-3 was low in CLL, HL, and
449 MM patients (2.4-4%) with a slightly elevated percentage of cells expressing these markers among the
450 DLBCL patients (9.9-22.8%). While KLRG-1 expression (~7.25%) was detectable in GF-CART01 patient cells,
451 it was significantly lower than KLRG-1 expression prior to nucleofection (~21.27%; p=0.0087)

452 **(Supplementary Figure S7A)**. The decrease in KLRG-1 expression was especially prominent in the CD8
453 population (52.50% vs. 14.59%; p=0.0004) **(Supplementary Figure S7B)**. A 48-hour cytotoxicity assay
454 further confirmed the functionality of the GF-CART01 cells **(Table 2)**. Together, our data suggest that the
455 *qCART*™ system is a promising technology for generating functional multiplex armored CAR-T_{SCM} cells for
456 cancer immunotherapy application. GF-CART01 therapy is a safe, potent, and cost-effective treatment for
457 B-cell malignancies.
458

459 **DISCUSSION/ CONCLUSION**

460 *qPB* is currently the most efficient transposon for gene integration, and GF-CART01 cell therapy
461 was the first CAR-T therapy developed using the *qPB*-based *qCART*™ system.[15,16] The *qCART*™ system
462 can easily produce CAR-T cells with transgene size >7.6 kb, which is not achievable by conventional
463 lentiviral/retroviral CAR-T engineering.[16] The limited cargo capacity of lentiviral/retroviral vector may
464 account for the lack of current CAR-T clinical trials targeting B-cell malignancies with both dual-targeting
465 and iCasp9 safety switch gene (5.2 kb transgene size) in the CAR design. In this report, we presented
466 evidence on the feasibility of manufacturing highly potent iCasp9-regulatable CD20/CD19-targeted CAR-
467 T_{SCM} cells using the virus-free *qCART*™ system for clinical application. We demonstrated the purity,
468 potency, and consistency profiles of CAR-T cells manufactured using the *qCART*™ system.

469 Maintaining sterility and controlling mycoplasma and endotoxin contamination in the CAR-T
470 product are important safety concerns. G-Rex is a GMP-compliant medical device used for cell
471 expansion.[19,20] The minimal manual operation of this device minimizes contamination risks.
472 Importantly, manufacturing GF-CART01 cells with G-Rex can be achieved without compromising CAR-T
473 efficacy. Consistent with our previous study, we observed low risk of genotoxicity in GF-CART01 cells,
474 given the safe integration profile, low enhancer activity, and low residual *qPBase*.[16] Acute toxicities in
475 CAR-T therapy-treated patients, such as CRS and ICANS, have been major concerns.[21–23] Furthermore,

476 a rare case of CAR^+ CD4 T cell lymphoma has been reported recently in patients treated with CD19 CAR-T
477 cells.[24,25] To safely manage toxicities, CAR-T cells can be eradicated by targeting CAR-T cells (e.g. anti-
478 EGFRt antibody) via antibody-dependent cellular cytotoxicity (ADCC) mechanism or using a small molecule
479 that activates a suicide gene introduced in the CAR design (e.g. iCasp9).[21] The ADCC approach has slower
480 onset of killing compared to the latter. We included an iCasp9 safety switch in our GF-CART01 design to
481 mitigate the adverse effects of CRS and ICANS. Indeed, Foster et al (2021) has recently demonstrated that
482 acute ICANS can be effectively controlled by treating CAR-T therapy patients with the iCasp9-activating
483 agent, rimiducid (AP1903).[26]

484 Manufacturing clinically relevant number of a pure high-quality CAR-T product is the first critical
485 step towards successful CAR-T therapy. One approach to expanding the CAR^+ T cell population is by
486 culturing with aAPC, but this often leads to a more differentiated and short-lived T_{EFF} or exhaustive CAR-T
487 phenotype.[27] Another approach is to include markers within the construct to enrich the CAR^+ T cell
488 population either via drug selection or antibody-mediated cell isolation during or after CAR-T *ex vivo*
489 expansion, respectively. However, such approaches increase the payload size and introduce
490 therapeutically irrelevant genes into the genome.[4,22,23] While we also used aAPC in our initial
491 experiments, we could generate sufficient quantity of patient-derived GF-CART01 cells without aAPC-
492 induced enrichment by addition of *Quantum Booster*™, a serum-free supplement which contains cellular
493 proteins and a set of cytokines with defined concentrations. These components of *Quantum Booster*™ act
494 to promote proliferation of the CAR-T cells while maintaining stemness as well as minimal levels of
495 senescence and exhaustion.[16] Notably, we have shown that *Quantum Booster*™ highly enriches CD4
496 T_{SCM}, which may be critical in maintaining $CD8^+$ CAR-T cells at the T_{SCM} differentiation stage while being
497 robustly expanded. Our recent study further confirmed that *qCART*™-manufactured CAR-T cells may be
498 more effective in tumor control without aAPC enrichment.[16] Here, we demonstrated that 2.29×10^8–
499 1.38×10^9 T cells could be generated in a 1 L-G-Rex within a short time-frame of 10 days using cancer

500 patient-derived T cells. Even at a low CAR^+ percentage of 20%, we could still produce sufficient number of
501 CAR^+ CAR-T cells ($4.58x10^6$–$2.76x10^7$) for treatment, and we can easily enrich CAR^+ T cells with aAPC should
502 the need arise.

503 The high potency of GF-CART01 cells can be attributed to the balanced CD8/CD4 CAR-T ratio and
504 the high enrichment of T_{SCM} in the engineered cells. It has been reported that a balanced CD8/CD4 CAR-T
505 ratio resulted in high remission rates.[28,29] To achieve this, others have engineered CD4 and CD8 CAR-T
506 cells separately before adoptive transfer.[28] While *qCART*™ cells derived from healthy donors generally
507 favored CD8 enrichment, cancer patient-derived *qCART*™ cells have a balanced CD8/CD4 CAR-T ratio
508 (**Figure 5)**. Thus, the *qCART*™ system naturally achieves the desired CD8/CD4 balance without the need to
509 engineer CD4 and CD8 CAR-T cells separately as seen in SB100X-modified CAR-T clinical trials.[30]

510 Our observation that, in contrast to a positive dose-dependent relationship between CD20 target
511 cell expression level and proliferation capacity of GF-CART01 cells, there appeared to be an inverse
512 association between CD19 target cell expression level and CAR-T proliferation when encountering K562
513 cells overexpressing different levels of CD19. However, potential toning of GF-CART01 cells would be
514 unlikely since we found CD19 expression level of Raji cell line was much lower than the K562 clone which
515 expressed the lowest level of CD19. In other words, since tumor's endogenous CD19 expression level was
516 generally lower than the level that can inhibit CAR-T proliferation, we do not expect to see a decrease in
517 CAR-T proliferation similar to that observed with the K562 CD19 overexpression clone which expressed
518 high levels of CD19.

519 T_{SCM} are a class of immunological memory critical for successful adoptive T cell therapies.[31–35]
520 The *qCART*™ system is unique in its ability to enrich T_{SCM} population without compromising the cell quality,
521 expansion, and production time of CAR-T cell product.[16] One approach to harness the potency of less-
522 differentiated T cells such as T_{SCM} is to shorten the *ex vivo* expansion time of CAR-T product. *Ghassemi et*
523 *al.* (2022) demonstrated that shortening the lentiviral CAR-T manufacturing process to 24-hours resulted

524 in a higher percentage of CAR-T cells with a memory phenotype.[36] Though these CAR-T cells displayed
525 stronger *in vivo* anti-tumor activity than their conventional counterpart, successful clinical translation of
526 this process remains to be demonstrated. Another approach is to culture CAR-T cells with specific
527 cytokines or chemical reagents.[34,35,37–39] Additionally, CAR-T cell production from defined T cell
528 subsets has been shown to be beneficial in enriching the T_{SCM} population.[40] However, none of these
529 approaches enrich T_{SCM} population to a high level seen in our *qCART*™-modified T cells. While T_{SCM} cells
530 make up a small percentage of T cells derived from cancer patients, genetically modifying these cells using
531 the *qCART*™ system resulted in enrichment of T_{SCM} to as high as >80% in both the CD4 and CD8 CAR^+ T cell
532 populations.

533 In conjunction with the ability of T_{SCM} to self-renew and persist long-term, we also observed low
534 expression of exhaustion (PD-1, TIM-3, and LAG-3) and senescence (CD57) biomarkers in our GF-CART01
535 cells **(Figure 2F-G; Table 2)**. KLRG-1 is a senescence marker. While we observed a small but significant
536 population of KLRG-1^+ cells in GF-CART01 cells, we also observed a significantly lower percentage of KLRG-
537 1^+ cells after CAR-T production compared to freshly isolated PBMCs **(Supplementary Figure S2)**. Herndler-
538 Brandstetter *et al.* (2018) recently described a class of memory T cell population developed from KLRG-1^+
539 effector CD8 T cells that have lost KLRG-1 expression.[31] These so-called "exKLRG-1 memory cells" have
540 been demonstrated to inhibit tumor growth more efficiently compared to KLRG-1^+ cells in an OT-I
541 melanoma mouse model. T_{SCM} cells generally lack KLRG-1 expression, and KLRG-1^+ T_{SCM} cells have been
542 associated with cancer patients undergoing relapse.[32,33] Given the significant decrease in KLRG-1
543 expression in GF-CART01 cells, it is possible that a significant proportion of CAR-T_{SCM} cells in our model
544 were actually exKLRG-1 memory cells. Thus, one possible mechanism that made it possible for *qCART*™
545 system to generate highly potent CAR-T_{SCM} cells may be through the conversion of KLRG-1^+ effector CD8
546 T cells to exKLRG-1 memory cells.

547 One of the major challenges of CAR-T cell manufacturing is the variation and inconsistency of CAR-
548 T cell products.[34] In one study of ten CLL and ALL patients, CAR-T cells expanded anywhere between
549 23.6 and 385-folds with retroviral CAR transduction of 4-70%.[35] Lentiviral transduction of 5.5-45.3% was
550 reported by other studies of CLL and ALL patients.[36,37] In our GF-CART01 study, we observed tighter
551 range of CAR^+ percentage (19.9-53.22%) and expansion (58.0-198.96 folds) among the eight cancer
552 patients **(Table 2)**. Furthermore, these low levels of variation were comparable to the CAR^+ percentage
553 (32.5-49.6%) and expansion (43.54-157.55 folds) among the healthy donors in our study, respectively.
554 More importantly, GF-CART01 cells derived from both healthy donors and patients can effectively
555 eradicate tumor cells.

556 In this study, we directly compared between the performance and anti-tumor efficacy of *qCART*™-
557 and lentivirally-engineered CAR-T cells in a solid tumor xenograft model. The results clearly demonstrated
558 superior performance, anti-tumor efficacy, and *in vivo* expansion of *qCART*™-produced CAR-T cells over
559 lentivirally-produced CAR-T cells (**Figure 4E-4G**). These observations suggest that *qCART*™-produced CAR-
560 T cells, including GF-CART01 cells, are indeed highly potent.

561 In summary, the *qCART*™ system is an elegant system for the manufacturing of CAR-T products.
562 In this study, we demonstrated that the *qCART*™ system can be used to produce patient-derived GF-
563 CART01 cells with all the desired attributes of CAR-T products to ensure therapeutic success, including
564 high CAR-$T_{SCM,}$ balanced CD8/CD4 ratio, low exhaustion and senescence marker expressions, high
565 expansion capacity, and excellent anti-tumor efficacy. We believe that the simplicity and robustness of
566 manufacturing multiplex CAR-T cells with enhanced product consistency using the *qCART*™ system will
567 not only significantly enhance the accessibility of CAR-T therapy but also unlock the full potential of
568 armored CAR-T therapy for the treatment of solid tumors in the future.

569

570

571 **REFERENCES**

572 1. Larson RC, Maus M V. Recent advances and discoveries in the mechanisms and functions of CAR
573 T cells. Nat Rev Cancer. Springer US; 2021;
574 2. Sheth VS, Gauthier J. Taming the beast: CRS and ICANS after CAR T-cell therapy for ALL. Bone
575 Marrow Transplant. Springer US; 2021;56:552 – 66.
576 3. Meir YJJ, Wu SCY. Transposon-based vector systems for gene therapy clinical Trials: Challenges
577 and considerations. Chang Gung Med J. 2011;34:565 – 79.
578 4. Singh H, Moyes JSE, Huls MH, Cooper LJN. Manufacture of T cells using the Sleeping Beauty
579 system to enforce expression of a CD19-specific chimeric antigen receptor. Cancer Gene Ther. Nature
580 Publishing Group; 2015;22:95 – 100.
581 5. Brentjens RJ, Latouche JB, Santos E, Marti F, Gong MC, Lyddane C, et al. Eradication of systemic
582 B-cell tumors by genetically targeted human T lymphocytes co-stimulated by CD80 and interleukin-
583 15. Nat Med. 2003;9:279 – 86.
584 6. Cronk RJ, Zurko J, Shah NN. Bispecific chimeric antigen receptor T cell therapy for b cell
585 malignancies and multiple myeloma. Cancers (Basel). 2020;12:1 – 15.
586 7. Levin A, Shah NN. Chimeric antigen receptor modified T cell therapy in B cell non-Hodgkin
587 lymphomas. Am J Hematol. 2019;94:S18 – 23.
588 8. Park JH, Rivière I, Gonen M, Wang X, Sénéchal B, Curran KJ, et al. Long-Term Follow-up of
589 CD19 CAR Therapy in Acute Lymphoblastic Leukemia. New England Journal of Medicine.
590 2018;378:449 – 59.
591 9. Spiegel JY, Dahiya S, Jain MD, Nastoupil LJ, Ghobadi A, Lin Y, et al. Outcomes in large B-cell
592 lymphoma progressing after axicabtagene ciloleucel (Axi-cel): Results from the U.S. Lymphoma
593 CAR-T Consortium. Journal of Clinical Oncology. 2019;37:7517 – 7517.
594 10. Neelapu SS, Rossi JM, Jacobson CA, Locke FL, Miklos DB, Reagan PM, et al. CD19-Loss with
595 Preservation of Other B Cell Lineage Features in Patients with Large B Cell Lymphoma Who
596 Relapsed Post-Axi-Cel. Blood. 2019;134:203 – 203.
597 11. Shah NN, Johnson BD, Schneider D, Zhu F, Szabo A, Keever-Taylor CA, et al. Bispecific anti-
598 CD20, anti-CD19 CAR T cells for relapsed B cell malignancies: a phase 1 dose escalation and
599 expansion trial. Nat Med. 2020;26:1569 – 75.
600 12. Tong C, Zhang Y, Liu Y, Ji X, Zhang WW, Guo Y, et al. Optimized tandem CD19/CD20 CAR-
601 engineered T cells in refractory/relapsed B cell lymphoma. Blood. 2020;136:1632 – 44.
602 13. Wu SCY, Meir YJJ, Coates CJ, Handler AM, Pelczar P, Moisyadi S, et al. piggyBac is a flexible
603 and highly active transposon as compared to Sleeping Beauty, Tol2, and Mos1 in mammalian cells.
604 Proc Natl Acad Sci U S A. 2006;103:15008 – 13.
605 14. Querques I, Mades A, Zuliani C, Miskey C, Alb M, Grueso E, et al. A highly soluble Sleeping
606 Beauty transposase improves control of gene insertion. Nat Biotechnol. Springer US; 2019;37:1502 –
607 12.
608 15. Hua W-K, Hsu JC, Chen Y-C, Chang PS, Wen KK-L, Wang P-N, et al. Quantum pBac: An
609 effective, high-capacity piggyBac-based gene integration vector system for unlocking gene therapy

610 potential. https://doi.org/101101/20220429490002 [Internet]. 2022; Available from:
611 https://doi.org/10.1101/2022.04.29.490002
612 16. Chen Y-C, Hua W-K, Hsu JC, Chang PS, Wen KK-L, Huang Y-W, et al. Quantum CART
613 (qCART), a piggyBac-based system for development and production of virus-free multiplex CAR-T
614 cell therapy. bioRxiv [Internet]. 2022; Available from: https://doi.org/10.1101/2022.05.03.490469
615 17. Hultin LE, Hausner MA, Hultin PM, Giorgi J v. Cd20 (pan-B cell) antigen is expressed at a low
616 level on a subpopulation of human T lymphocytes. Cytometry. 1993;14:196 – 204.
617 18. Nicholson IC, Lenton KA, Little DJ, Decorso T, Lee FT, Scott AM, et al. Construction and
618 characterisation of a functional CD19 specific single chain Fv fragment for immunotherapy of B
619 lineage leukaemia and lymphoma. Mol Immunol. 1997;34:1157 – 65.
620 19. Gotti E, Tettamanti S, Zaninelli S, Cuofano C, Cattaneo I, Rotiroti MC, et al. Optimization of
621 therapeutic T cell expansion in G-Rex device and applicability to large-scale production for clinical
622 use: GMP-compliant polyclonal T cell expansion in G-Rex. Cytotherapy. 2022;24:334 – 43.
623 20. Gagliardi C, Khalil M, Foster AE. Streamlined production of genetically modified T cells with
624 activation, transduction and expansion in closed-system G-Rex bioreactors. Cytotherapy. Elsevier Inc.;
625 2019;21:1246 – 57.
626 21. Rafiq S, Hackett CS, Brentjens RJ. Engineering strategies to overcome the current roadblocks in
627 CAR T cell therapy. Nat Rev Clin Oncol. Springer US; 2020;17:147 – 67.
628 22. Wang X, Chang WC, Wong CLW, Colcher D, Sherman M, Ostberg JR, et al. A transgene-
629 encoded cell surface polypeptide for selection, in vivo tracking, and ablation of engineered cells.
630 Blood. 2011;118:1255 – 63.
631 23. Wang Q, He F, He W, Huang Y, Zeng J, Zi F, et al. A transgene-encoded truncated human
632 epidermal growth factor receptor for depletion of anti- B-cell maturation antigen CAR-T cells. Cell
633 Immunol. Elsevier Inc.; 2021;363:104342.
634 24. Micklethwaite KP, Gowrishankar K, Gloss BS, Li Z, Street JA, Moezzi L, et al. Investigation of
635 product-derived lymphoma following infusion of piggyBac-modified CD19 chimeric antigen receptor
636 T cells. Blood. American Society of Hematology; 2021;138:1391 – 405.
637 25. Bishop DC, Clancy LE, Simms R, Burgess J, Mathew G, Moezzi L, et al. Development of CAR
638 T-cell lymphoma in 2 of 10 patients effectively treated with piggyBac-modified CD19 CAR T cells.
639 Blood. American Society of Hematology; 2021;138:1504 – 9.
640 26. Foster MC, Savoldo B, Lau W, Rubinos C, Grover N, Armistead P, et al. Utility of a safety switch
641 to abrogate CD19.CAR T-cell – associated neurotoxicity. Blood. 2021;137:3306 – 9.
642 27. Nukala U, Rodriguez Messan M, Yogurtcu ON, Wang X, Yang H. A Systematic Review of the
643 Efforts and Hindrances of Modeling and Simulation of CAR T-cell Therapy. AAPS Journal.
644 2021;23:1 – 33.
645 28. Turtle CJ, Hanafi LA, Berger C, Gooley TA, Cherian S, Hudecek M, et al. CD19 CAR-T cells of
646 defined CD4+:CD8+ composition in adult B cell ALL patients. Journal of Clinical Investigation.
647 2016;126:2123 – 38.
648 29. Sommermeyer D, Hudecek M, Kosasih PL, Gogishvili T, Maloney DG, Turtle CJ, et al. Chimeric
649 antigen receptor-modified T cells derived from defined CD8+ and CD4+ subsets confer superior
650 antitumor reactivity in vivo. Leukemia. 2016;30:492 – 500.

651 30. Prommersberger S, Reiser M, Beckmann J, Danhof S, Amberger M, Quade-Lyssy P, et al.
652 CARAMBA: a first-in-human clinical trial with SLAMF7 CAR-T cells prepared by virus-free
653 Sleeping Beauty gene transfer to treat multiple myeloma. Gene Ther. Springer US; 2021;28:560 – 71.
654 31. Herndler-Brandstetter D, Ishigame H, Shinnakasu R, Plajer V, Stecher C, Zhao J, et al. KLRG1+
655 Effector CD8+ T Cells Lose KLRG1, Differentiate into All Memory T Cell Lineages, and Convey
656 Enhanced Protective Immunity. Immunity. Elsevier Inc.; 2018;48:716-729.e8.
657 32. Liu Q, Sun Z, Chen L. Memory T cells: strategies for optimizing tumor immunotherapy. Protein
658 Cell. Higher Education Press; 2020;11:549 – 64.
659 33. Noviello M, Manfredi F, Ruggiero E, Perini T, Oliveira G, Cortesi F, et al. Bone marrow central
660 memory and memory stem T-cell exhaustion in AML patients relapsing after HSCT. Nat Commun.
661 2019;10:1 – 15.
662 34. Vormittag P, Gunn R, Ghorashian S, Veraitch FS. A guide to manufacturing CAR T cell therapies.
663 Curr Opin Biotechnol. Elsevier Ltd; 2018;53:164 – 81.
664 35. Brentjens RJ, Rivière I, Park JH, Davila ML, Wang X, Stefanski J, et al. Safety and persistence of
665 adoptively transferred autologous CD19-targeted T cells in patients with relapsed or chemotherapy
666 refractory B-cell leukemias. Blood. 2011;118:4817 – 28.
667 36. Porter DL, Hwang WT, Frey N V., Lacey SF, Shaw PA, Loren AW, et al. Chimeric antigen
668 receptor T cells persist and induce sustained remissions in relapsed refractory chronic lymphocytic
669 leukemia. Sci Transl Med. 2015;7.
670 37. Dai H, Zhang W, Li X, Han Q, Guo Y, Zhang Y, et al. Tolerance and efficacy of autologous or
671 donor-derived T cells expressing CD19 chimeric antigen receptors in adult B-ALL with
672 extramedullary leukemia. Oncoimmunology. 2015;4.
673
674
675
676
677
678
679
680
681
682
683

684 **FIGURE LEGENDS**

685 **Figure 1. Comparison of perfusion and fed-batch-cultured CAR-T cells.** (A) Schematic diagram of the GF-
686 CART01 CAR construct. A T2A sequence enables co-expression of iCasp9 and CD20/CD19-targeted scFvs
687 under the EF1α promoter. (B) Characterization of GF-CART01 cells cultured in conventional plates
688 (perfusion) or G-Rex (fed batch) at day 10 after nucleofection. (C) Cytolytic activities of CAR-T cells after
689 48 or 72 h of co-culture with Raji-GFP/Luc target cells (E:T ratio of 5:1) were assessed by Celigo image
690 cytometry. (B-C) Data represent mean ± SD in 6 healthy donors, n=6. *p<0.05, ***p*<0.01, ****p*<0.001.

691

692 **Figure 2. Characteristics of GF-CART01 cells.** Percentage of (A) CAR^+ and (B) $transposase^+$ (*qPBase*$^+$) cells
693 were analyzed by flow cytometry on days 1, 8, and 10 after nucleofection. (C) Fold change of GF-CART01
694 cells after 10 days of culture in G-Rex are shown. (D) Percentage of CD4 and CD8 T cells in the CAR^+
695 population on day 10 after nucleofection. (E) Distribution of T_N, T_{SCM}, T_{CM}, T_{EM}, and T_{EFF} subsets in the CD4
696 (upper panel) and CD8 populations (lower panel). (F) Expression of exhaustion markers PD-1, TIM-3, and
697 LAG-3 in GF-CART01 cells. (G) Expression of senescence markers KLRG-1 and CD57 in GF-CART01 cells. (A-
698 G) Data represent mean ± SD in 9 healthy donors, n=9. Each set of histogram plots shown in (D), (E), (F),
699 and (G) represents one donor.

700

701 **Figure 3. *In vitro* functional analysis of GF-CART01 cells.** (A-B) CAR-T cells derived from two healthy
702 donors PBMC-41 and PBMC-40 were assessed for cytotoxicity against Raji-GFP/Luc cells by Celigo image
703 cytometry. Statistical differences were calculated by One-way ANOVA with Tukey multiple comparison,
704 ****p*<0.001, ***p*<0.01, **p*<0.05. (C) IFN-γ, (D) TNF-α, and (E) IL-2 secretion by GF-CART01 cells following
705 antigen stimulation was determined by ELISA. Pan-T cells (non-modified cells) served as a control group.
706 Data represent mean ± SD, n=3. Statistical differences are calculated by Student's t-test, ****p*<0.001.

707

708 **Figure 4. Anti-tumor activity of GF-CART01 cells in a B-cell lymphoma immunodeficient xenograft mouse**
709 **model.** (A) Schematic diagram of *in vivo* Raji xenograft model experimental design. (B-C) Bioluminescent
710 imaging was performed to monitor tumor cell persistence (n= 4/group) and tumor growth were quantified
711 by total flux (photon/s). (D) Kaplan-Meier survival curves for the different treatment groups are shown.
712 (E) Schematic diagram of *in vivo* NCI-N87 xenograft model experimental design. (F) Bioluminescent
713 imaging was performed to monitor tumor cell persistence (n= 3/group). (G) Human T cell counts of blood
714 samples taken from the indicated group of mice at Day 21 and Day 48 post-tumor inoculation.
715
716 **Figure 5. Assessment of cancer-patient-derived GF-CART01 cells.** T cells derived from healthy donors and
717 cancer patients were nucleofected with GF-CART01. (A) CD8/CD4 ratios were assessed before (PBMC) and
718 after (CAR-T) nucleofection. (B) Distribution of T_N, T_{SCM}, T_{CM}, T_{EM}, and T_{EFF} subsets in $CD4^+$ (upper panel)
719 and $CD8^+$ (lower panel) CAR-T cell populations. DLBCL, diffuse large B-cell lymphoma; CLL, chronic
720 lymphocytic leukemia; HL, Hodgkin's lymphoma; MM, multiple myeloma.
721
722

Figure 1.

A

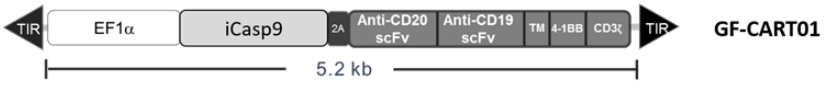

GF-CART01

B

Culture Vessel	Conventional Plate (perfusion)	G-Rex (fed batch)
% CAR⁺ T cells	51%* (44%~61%, n=6)	46%* (42%~49%, n=6)
Expansion capacity of CAR⁺ T cells	836 fold* (406~2090 fold, n=6)	189 fold* (139~262 fold, n=6)
Distribution of T cell subsets in CAR⁺ T cells	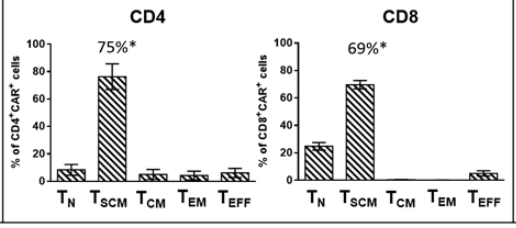	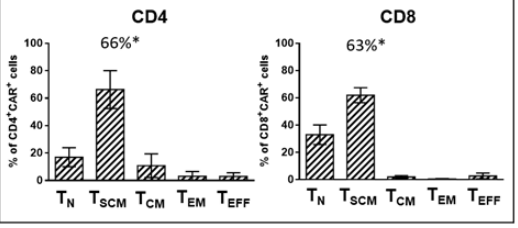

*median

C

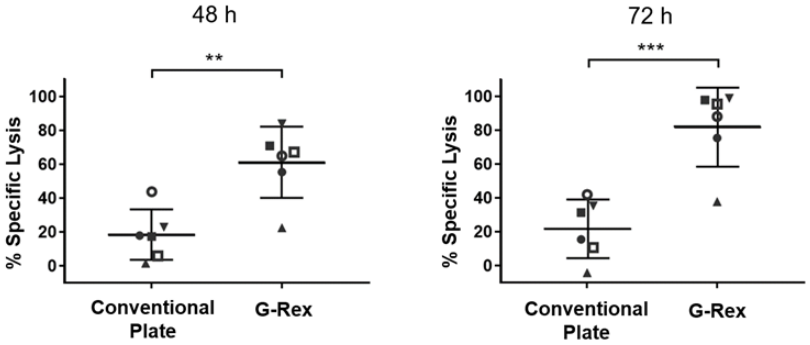

723

724

Figure 2.

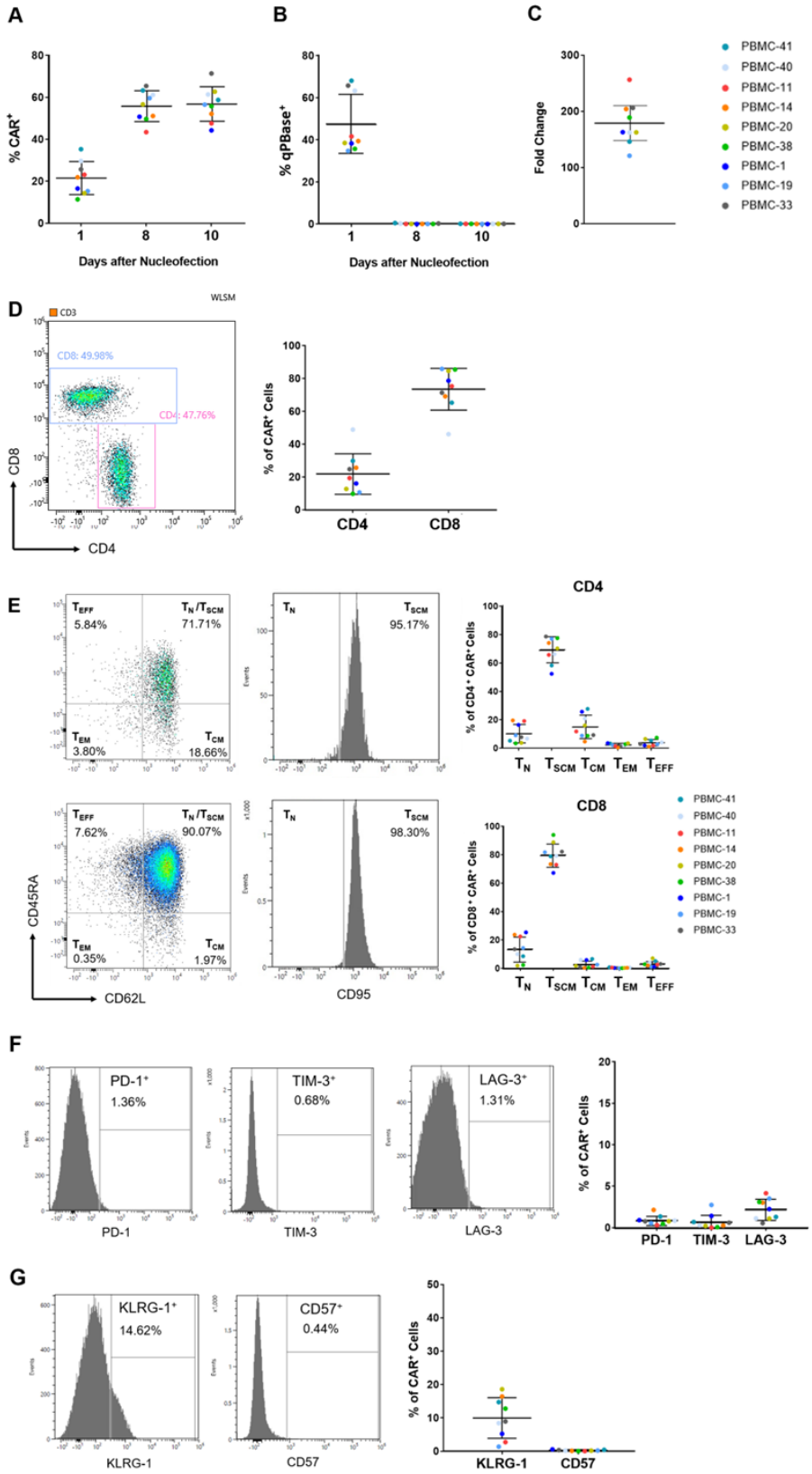
A
% CAR+
Days after Nucleofection
B
% qPBase+
Days after Nucleofection
C
Fold Change
PBMC-41
PBMC-40
PBMC-11
PBMC-14
PBMC-20
PBMC-38
PBMC-1
PBMC-19
PBMC-33
D
CD3
CD8: 49.98%
CD4: 47.76%
CD8
CD4
% of CAR+ Cells
CD4
CD8
E
TEFF 5.84%
TN/TSCM 71.71%
TEM 3.80%
TCM 18.66%
TN
TSCM 95.17%
% of CD4+ CAR+ Cells
CD4
TN TSCM TCM TEM TEFF
TEFF 7.62%
TN/TSCM 90.07%
TEM 0.35%
TCM 1.97%
CD45RA
CD62L
TN
TSCM 98.30%
CD95
% of CD8+ CAR+ Cells
CD8
TN TSCM TCM TEM TEFF
PBMC-41
PBMC-40
PBMC-11
PBMC-14
PBMC-20
PBMC-38
PBMC-1
PBMC-19
PBMC-33
F
PD-1+ 1.36%
PD-1
TIM-3+ 0.68%
TIM-3
LAG-3+ 1.31%
LAG-3
% of CAR+ Cells
PD-1 TIM-3 LAG-3
G
KLRG-1+ 14.62%
KLRG-1
CD57+ 0.44%
CD57
% of CAR+ Cells
KLRG-1 CD57

725

Figure 3.

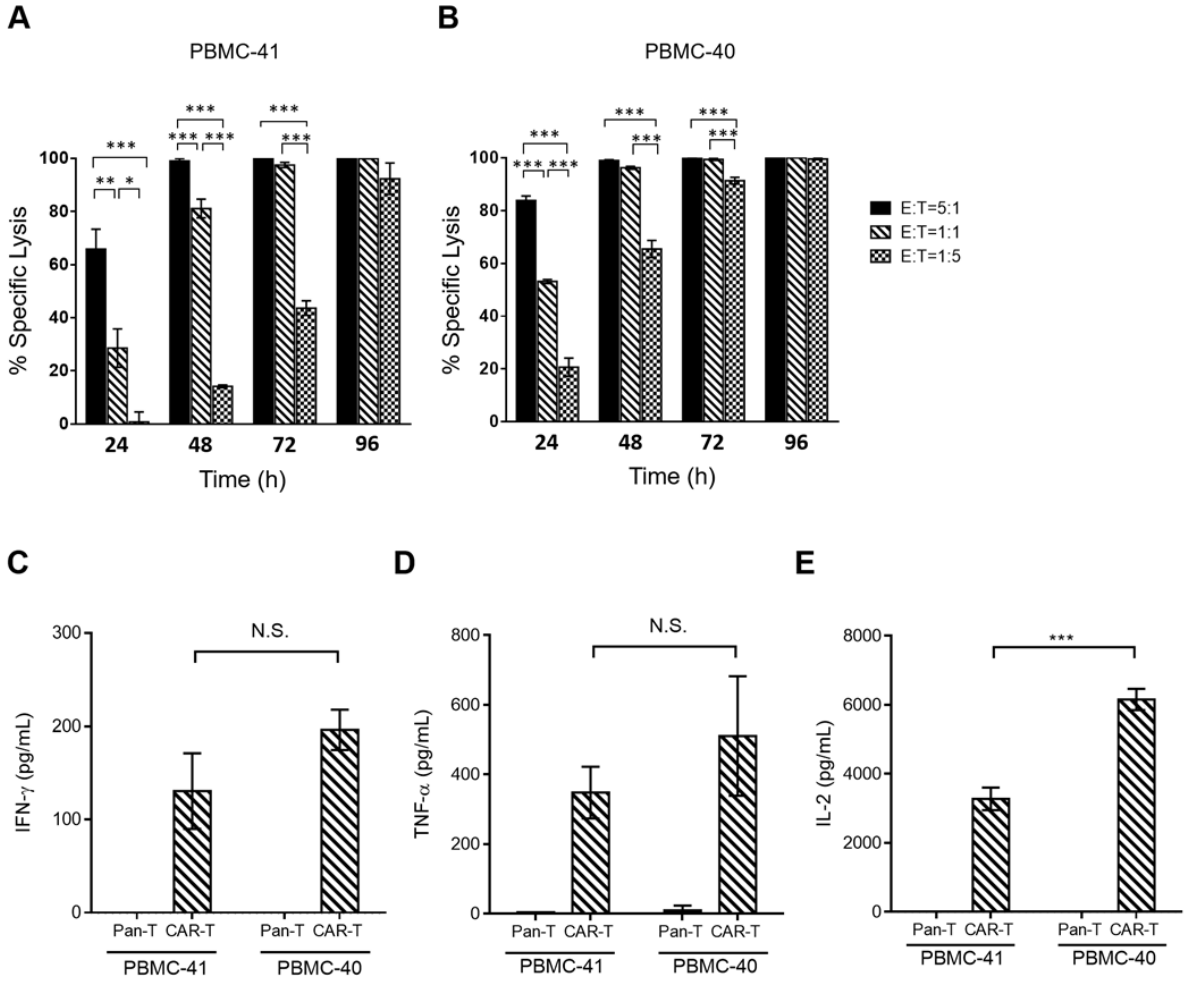
A
PBMC-41
% Specific Lysis
Time (h)
B
PBMC-40
% Specific Lysis
Time (h)
E:T=5:1
E:T=1:1
E:T=1:5
C
IFN-γ (pg/mL)
N.S.
D
TNF-α (pg/mL)
N.S.
E
IL-2 (pg/mL)
Pan-T
CAR-T
PBMC-41
PBMC-40

726

Figure 4.

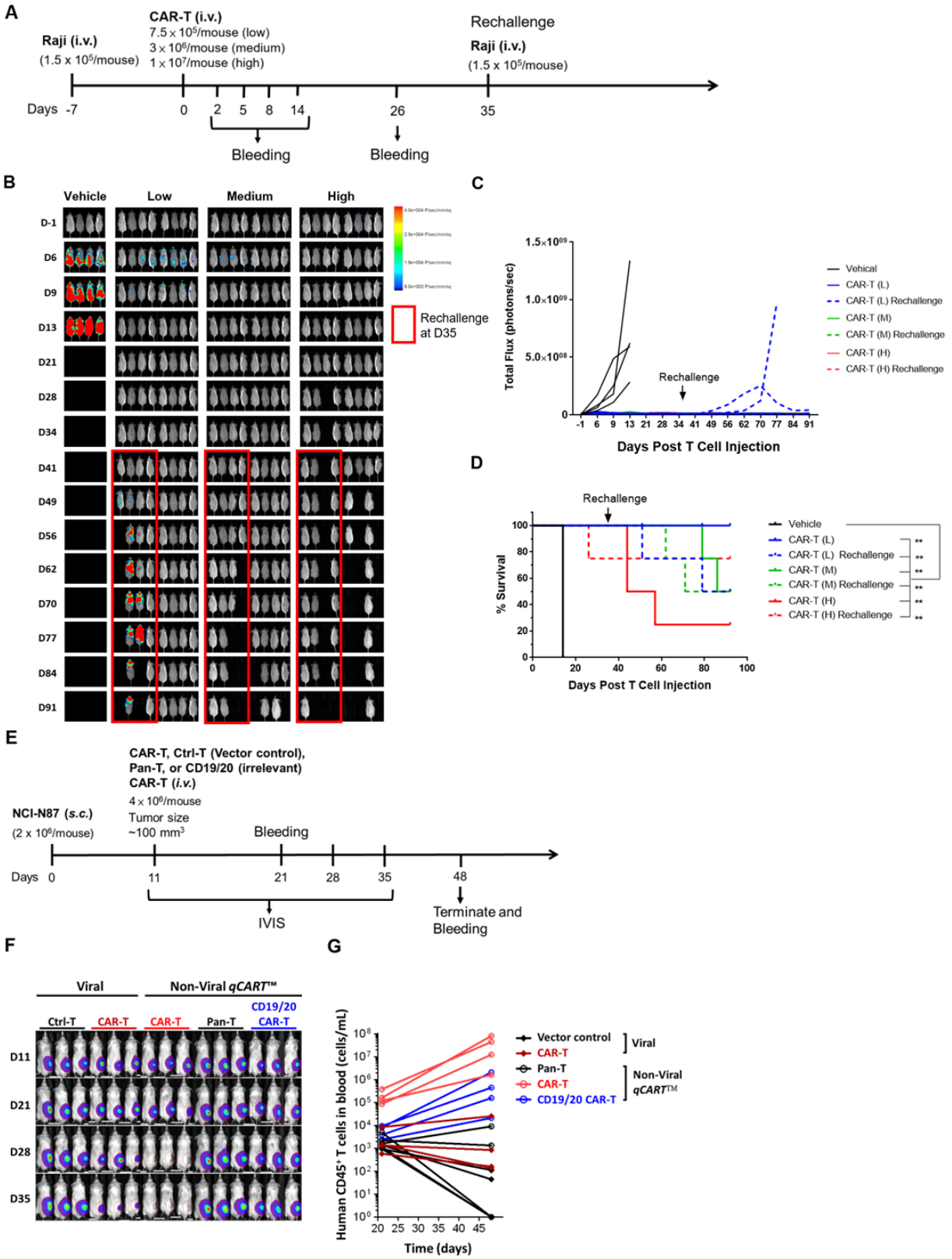
A
Raji (i.v.)
(1.5 x 10^5/mouse)
CAR-T (i.v.)
7.5 x 10^5/mouse (low)
3 x 10^6/mouse (medium)
1 x 10^7/mouse (high)
Rechallenge
Raji (i.v.)
(1.5 x 10^5/mouse)
Days -7
0
2 5 8 14
26
35
Bleeding
Bleeding
B
Vehicle
Low
Medium
High
D-1
D6
D9
D13
D21
D28
D34
D41
D49
D56
D62
D70
D77
D84
D91
Rechallenge at D35
C
Total Flux (photons/sec)
1.5×10^09
1.0×10^09
5.0×10^08
0
Rechallenge
-1 6 9 13 21 28 34 41 49 56 62 70 77 84 91
Days Post T Cell Injection
Vehical
CAR-T (L)
CAR-T (L) Rechallenge
CAR-T (M)
CAR-T (M) Rechallenge
CAR-T (H)
CAR-T (H) Rechallenge
D
Rechallenge
% Survival
100
80
60
40
20
0
0 20 40 60 80 100
Days Post T Cell Injection
Vehicle
CAR-T (L)
CAR-T (L) Rechallenge
CAR-T (M)
CAR-T (M) Rechallenge
CAR-T (H)
CAR-T (H) Rechallenge
**
E
NCI-N87 (s.c.)
(2 x 10^6/mouse)
CAR-T, Ctrl-T (Vector control),
Pan-T, or CD19/20 (irrelevant)
CAR-T (i.v.)
4 x 10^6/mouse
Tumor size
~100 mm^3
Bleeding
Days 0
11
21
28
35
48
IVIS
Terminate and
Bleeding
F
Viral
Non-Viral qCART™
Ctrl-T
CAR-T
CAR-T
Pan-T
CD19/20
CAR-T
D11
D21
D28
D35
G
Human CD45+ T cells in blood (cells/mL)
10^8
10^7
10^6
10^5
10^4
10^3
10^2
10^1
10^0
20 25 30 35 40 45
Time (days)
Vector control
CAR-T
Viral
Pan-T
CAR-T
CD19/20 CAR-T
Non-Viral
qCART™

727

Figure 5.

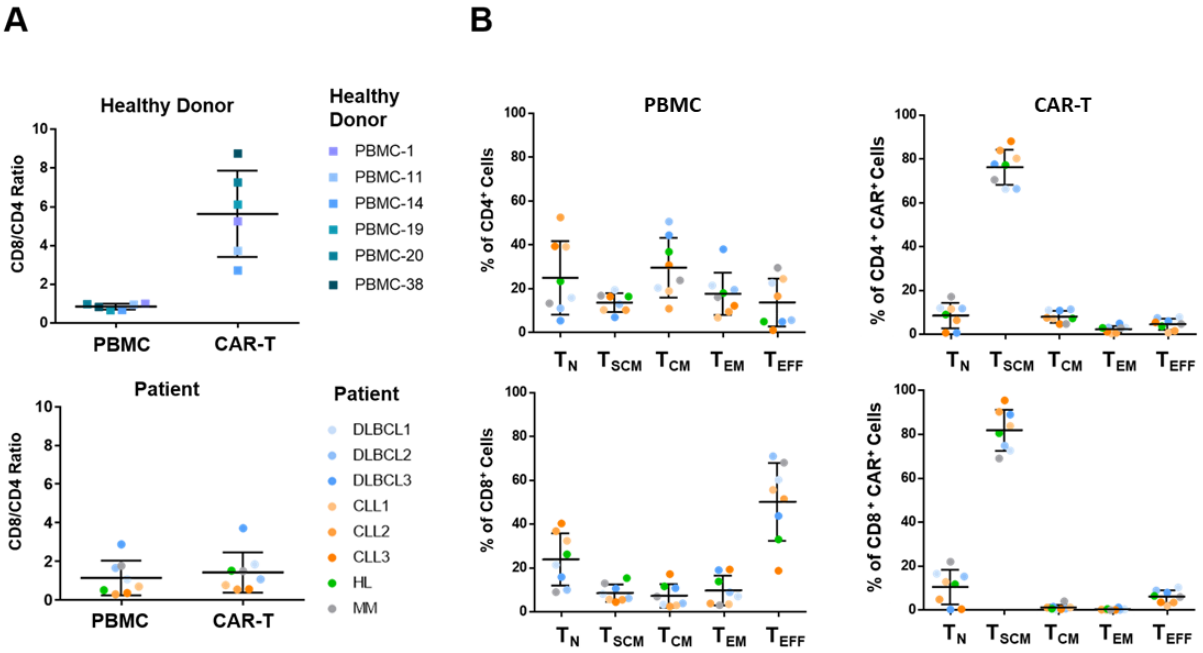
A
B
Healthy Donor
CD8/CD4 Ratio
PBMC
CAR-T
Healthy Donor
PBMC-1
PBMC-11
PBMC-14
PBMC-19
PBMC-20
PBMC-38
Patient
DLBCL1
DLBCL2
DLBCL3
CLL1
CLL2
CLL3
HL
MM
PBMC
CAR-T
% of CD4+ Cells
% of CD8+ Cells
% of CD4+ CAR+ Cells
% of CD8+ CAR+ Cells
TN
TSCM
TCM
TEM
TEFF

728